AD NUMBER

AD801784

LIMITATION CHANGES

TO:

Approved for public release; distribution is unlimited.

FROM:

Distribution authorized to U.S. Gov't. agencies and their contractors; Administrative/Operational Use; JUL 1959. Other requests shall be referred to Army Bllistic Research Laboratory, Aberdeen Proving Ground, MD 21005.

AUTHORITY

BRL D/A ltr, 22Apr 1981

BRL

REPORT NO. 1078
JULY 1959

A METHOD FOR MEASURING DAMPING-IN-PITCH OF MODELS IN SUPERSONIC FLOW

H. E. MALOY, Jr.

DEPARTMENT OF THE ARMY PROJECT NO. 503-03-009
ORDNANCE RESEARCH AND DEVELOPMENT PROJECT NO. TB1-0014
BALLISTIC RESEARCH LABORATORIES
ABERDEEN PROVING GROUND, MARYLAND

Destroy when no longer needed. DO NOT RETURN

SUPPLEMENT TO BRL REPORT NO. 1078

FEBRUARY 1960

NOTES ON THE APPLICATION OF MUNK'S THEORY TO DAMPING-IN-PITCH OF BODIES OF REVOLUTION IN SUPERSONIC FLOW

H. P. Hitchcock

The Appendix to H. E. Maloy, Jr's report, "A Method for Measuring Damping-in-Pitch of Models in Supersonic Flow," has some typographical errors that need to be corrected, and also requires some explanation to make its meaning clear.

In the equation after (8), "u" should be "U". In the next equation, "$\frac{\partial s}{\partial x}$" should be "$\frac{\partial S}{\partial x}$". In equation (10), the first term of the right member should be negative and the last bracket should be placed at the end of the equation. The right member of the equation for $\dot{\delta}$ should be negative. Incidentally, there is not distinction between this δ and the α_s used previously; in the main report, this angle is denoted by α.

The cross sectional area S, introduced in equation (6), is a function of the axial distance x from the center of gravity of the body. At the nose, $x = x_n$ and $S = 0$. At the base, $x = x_b$ and $S = S_b$.

The static angle of attack is α_s. But if the axis of the body has an angular velocity of rotation, Ω, each point on the axis has an additional velocity Ωx, as shown by (7), and this produces an additional angle of attack

$$\alpha_\omega = \frac{\Omega x}{U} ,$$

where U is the free stream velocity. The figure should show that α_s and Ω are positive in a clockwise direction.

It is assumed that the projectile oscillates harmonically, so that

$$\alpha_s = A \cos \omega t, \quad \dot{\alpha}_s = - A\omega \sin \omega t, \quad \ddot{\alpha}_s = - A\omega^2 \cos \omega t.$$

This assumption is convenient, but the same result could be obtained without it. Now, since $\Omega = \dot{\alpha}_s$,

$$\alpha_\omega = -A\omega \frac{x}{U} \sin \omega t, \quad \dot{\alpha}_\omega = - A\omega^2 \frac{x}{U} \cos \omega t.$$

Now considering equation (10), the moment over the whole body is

$$M = \rho U \int_{x_n}^{x_b} \left[S\left(-A\omega x \sin \omega t - \frac{A\omega^2 x^2}{U} \cos \omega t\right) + (AUx \cos \omega t - A\omega x^2 \sin \omega t)S' - SA\omega x \sin \omega t \right] dx,$$

where ρ denotes the air density, and $S' = \frac{\partial S}{\partial x}$.

The moment of inertia of the displaced air with respect to a transverse plane through the center of gravity is defined as

$$I_{cg} = \rho \int_{x_n}^{x_b} x^2 S \, dx.$$

The volume of the body is

$$V = \int_{x_n}^{x_b} S \, dx.$$

Integrating by parts, we find that

$$\int_{x_n}^{x_b} xS' \, dx = x_b S_b - V,$$

$$\int_{x_n}^{x_b} x^2 S' \, dx = x_b^2 S_b - 2 \int_{x_n}^{x_b} xS \, dx.$$

Hence, the equation for M assumes the form of equation (10).

Now the spring constant is

$$k = \rho U^2 (x_b S_b - V),$$

and the damping factor is

$$\mu_o = \rho U x_b^2 S b.$$

Making these substitutions and using the expressions for α_s and its derivatives, we obtain the equation

$$M = I_{cg} \ddot{\alpha}_s + \mu_o \dot{\alpha}_s + k\alpha_s.$$

In the present connection, it is appropriate to call $\mu_o \dot{\alpha}_s$ the damping moment. However, in the theory of spinning shell, the rolling moment and the Magnus moment also tend to damp the yaw.[1] Therefore, it is preferable to call the term due to yawing the yawing moment.

Since Munk's theory neglects viscosity and compressibility, it could not be expected to give reliable results at supersonic Mach numbers. However, T. L. Smith has pointed out that the theory which was first used for dirigible balloons might predict the right order of magnitude of the yawing moment coefficient K_H for small angles of attack, providing the cross-flow (normal to the axis of the shell) is subsonic. In the present case, it did, although the theoretical result is less than the experimental values, which are given in Table I of Maloy's report.

A closer estimate is obtained by the empirical formula, which was determined from firings of projectiles from caliber 0.30 to 37mm at velocities from 2000 to 3050 feet per second:

$$K_H = 0.35\ L^{1.5},$$

---

[1] Kent, R. H. "Notes on a Theory of Spinning Shell" APG: BRL Report No. 898, 1954. See Eq. (15). After Fowler, Kent uses the cumbersome name, 'yawing moment due to yawing'.

where L is the length of the projectile in calibers.[2] For a 5-caliber projectile, this formula gives $K_H = 3.91$, which is 6% less than the mean experimental value at M = 3.0 and 5% more than the mean at M = 4.0.

It should be noted that the experimental values decrease with Mach number. The following table exhibits the averages.

Mach No.	No. of Observations	K_H
1.75	1	5.23
2.50	1	4.37
3.00	5	4.155
4.00	5	3.72
4.50	2	3.35

H. P. HITCHCOCK

[2] Hitchcock, H. P. "Aerodynamic Data for Spinning Projectiles." APG: BRL Report No. 620, 1947. See page 13.

SUPPLEMENT TO BRL REPORT NO. 1078

FEBRUARY 1960

NOTES ON THE APPLICATION OF MUNK'S THEORY TO DAMPING-IN-PITCH OF BODIES OF REVOLUTION IN SUPERSONIC FLOW

H. P. Hitchcock

The Appendix to H. E. Maloy, Jr's report, "A Method for Measuring Damping-in-Pitch of Models in Supersonic Flow," has some typographical errors that need to be corrected, and also requires some explanation to make its meaning clear.

In the equation after (8), "u" should be "U". In the next equation, $\frac{\partial s}{\partial x}$ should be $\frac{\partial S}{\partial x}$. In equation (10), the first term of the right member should be negative and the last bracket should be placed at the end of the equation. The right member of the equation for $\dot{\delta}$ should be negative. Incidentally, there is not distinction between this δ and the α_s used previously; in the main report, this angle is denoted by α.

The cross sectional area S, introduced in equation (6), is a function of the axial distance x from the center of gravity of the body. At the nose, $x = x_n$ and $S = 0$. At the base, $x = x_b$ and $S = S_b$.

The static angle of attack is α_s. But if the axis of the body has an angular velocity of rotation, Ω, each point on the axis has an additional velocity Ωx, as shown by (7), and this produces an additional angle of attack

$$\alpha_\omega = \frac{\Omega x}{U} ,$$

where U is the free stream velocity. The figure should show that α_s and Ω are positive in a clockwise direction.

It is assumed that the projectile oscillates harmonically, so that

$$\alpha_s = A \cos \omega t, \quad \dot{\alpha}_s = - A\omega \sin \omega t, \quad \ddot{\alpha}_s = - A\omega^2 \cos \omega t.$$

This assumption is convenient, but the same result could be obtained without it. Now, since $\Omega = \dot{\alpha}_s$,

$$\alpha_\omega = -A\omega \frac{x}{U} \sin \omega t, \quad \dot{\alpha}_\omega = - A\omega^2 \frac{x}{U} \cos \omega t.$$

Now considering equation (10), the moment over the whole body is

$$M = \rho U \int_{x_n}^{x_b} \left[S\left(-A\omega x \sin \omega t - \frac{A\omega^2 x^2}{U} \cos \omega t\right) + (AUx \cos \omega t - A\omega x^2 \sin \omega t) S' - SA\omega x \sin \omega t \right] dx,$$

where ρ denotes the air density, and $S' = \frac{\partial S}{\partial x}$.

The moment of inertia of the displaced air with respect to a transverse plane through the center of gravity is defined as

$$I_{cg} = \rho \int_{x_n}^{x_b} x^2 S \, dx.$$

The volume of the body is

$$V = \int_{x_n}^{x_b} S \, dx.$$

Integrating by parts, we find that

$$\int_{x_n}^{x_b} xS' \, dx = x_b S_b - V,$$

$$\int_{x_n}^{x_b} x^2 S' \, dx = x_b^2 S_b - 2 \int_{x_n}^{x_b} xS \, dx.$$

Hence, the equation for M assumes the form of equation (10).

Now the spring constant is

$$k = \rho U^2 (x_b S_b - V),$$

and the damping factor is

$$\mu_o = \rho U x_b^2 S b.$$

Making these substitutions and using the expressions for α_s and its derivatives, we obtain the equation

$$M = I_{cg} \ddot{\alpha}_s + \mu_o \dot{\alpha}_s + k\alpha_s.$$

In the present connection, it is appropriate to call $\mu_o \dot{\alpha}_s$ the damping moment. However, in the theory of spinning shell, the rolling moment and the Magnus moment also tend to damp the yaw.[1] Therefore, it is preferable to call the term due to yawing the yawing moment.

Since Munk's theory neglects viscosity and compressibility, it could not be expected to give reliable results at supersonic Mach numbers. However, T. L. Smith has pointed out that the theory which was first used for dirigible balloons might predict the right order of magnitude of the yawing moment coefficient K_H for small angles of attack, providing the cross-flow (normal to the axis of the shell) is subsonic. In the present case, it did, although the theoretical result is less than the experimental values, which are given in Table I of Maloy's report.

A closer estimate is obtained by the empirical formula, which was determined from firings of projectiles from caliber 0.30 to 37mm at velocities from 2000 to 3050 feet per second:

$$K_H = 0.35\ L^{1.5},$$

---

[1] Kent, R. H. "Notes on a Theory of Spinning Shell" APG: BRL Report No. 898, 1954. See Eq. (15). After Fowler, Kent uses the cumbersome name, 'yawing moment due to yawing'.

where L is the length of the projectile in calibers.[2] For a 5-caliber projectile, this formula gives $K_H = 3.91$, which is 6% less than the mean experimental value at M = 3.0 and 5% more than the mean at M = 4.0.

It should be noted that the experimental values decrease with Mach number. The following table exhibits the averages.

Mach No.	No. of Observations	K_H
1.75	1	5.23
2.50	1	4.37
3.00	5	4.155
4.00	5	3.72
4.50	2	3.35

H. P. HITCHCOCK

[2] Hitchcock, H. P. "Aerodynamic Data for Spinning Projectiles." APG: BRL Report No. 620, 1947. See page 13.

B A L L I S T I C R E S E A R C H L A B O R A T O R I E S

REPORT NO. 1078

JULY 1959

A METHOD FOR MEASURING DAMPING-IN-PITCH OF MODELS IN SUPERSONIC FLOW

H. E. Maloy, Jr.

Department of the Army Project No. 503-03-009
Ordnance Research and Development Project No. TB3-1838

A B E R D E E N P R O V I N G G R O U N D, M A R Y L A N D

TABLE OF CONTENTS

Page

ABSTRACT. 3

DEFINITION OF SYMBOLS 5

LIST OF FIGURES 7

I. INTRODUCTION. 9

II. EXPERIMENTAL PROCEDURE. 10

A. Model Support and Recording System 10

B. Reduction of Data. 12

C. Windtunnel 15

III. CONCLUSIONS 16

IV. APPENDIX. 17

V. REFERENCES. 19

VI. TABLES. 20

VII. FIGURES 21

B A L L I S T I C R E S E A R C H L A B O R A T O R I E S

REPORT NO. 1078

HEMaloy, Jr./djp
Aberdeen Proving Ground, Md.
July 1959

A METHOD FOR MEASURING DAMPING-IN-PITCH OF MODELS IN SUPERSONIC FLOW

ABSTRACT

A technique has been developed to measure the damping-in-pitch of bodies of revolution in the Supersonic Wind Tunnel over a Mach number range of 1.75 to 4.5. The angular position of the model at any time is recorded with an oscillograph. The aerodynamic damping moments are computed from measurements of the rate of subsidence of the angle of attack.

ACKNOWLEDGMENTS

The author wishes to express his appreciation to Drs. J. Sternberg and T. Smith for their assistance in preparing this report and to Corporals M. Dustin and E. Lower for their help with the many details associated with the program.

DEFINITION OF SYMBOLS

d	=	diameter of model
k	=	restoring moment per unit angular deflection
q	=	dynamic pressure
t	=	time
u	=	free stream velocity
C.G.	=	center of gravity
I	=	moment of inertia
K_H	=	damping coefficient
M	=	Mach number
P_O	=	supply pressure
Re	=	Reynolds number
T_O	=	supply temperature
α	=	angle of attack
ρ	=	air density
μ	=	damping moment per time rate of change of angle of attack
ω	=	angular frequency of oscillation

LIST OF FIGURES

Fig. 1 Drawing of model

Fig. 2 Drawing of flexures

Fig. 3 Drawing of one piece flexure unit

Fig. 4 Drawing of model support system

Fig. 5 Wiring diagram

Fig. 6 Photograph of model and support system

Fig. 7 Reproduction of typical oscillograph record

Fig. 8 Semi-logarithmic plot of oscillograph record

Fig. 9 Graph of mechanical damping versus oscillatory frequency

Fig. 10 Graph of aerodynamic damping coefficient K_H vs Mach number

Fig. 11 Shadowgraph of flow with and without turbulence promoter at $\alpha = 0^\circ$

Fig. 12 Shadowgraph of flow with and without turbulence promoter at $\alpha = 2^\circ$

Fig. 13 Schlieren pictures of flow around model

Fig. 14 Reproduction of an oscillograph record showing flow disturbance in Tunnel No. 3 at Mach 1.73

Fig. 15 Reproduction of an oscillograph record showing absence of flow disturbance in Tunnel No. 1 at Mach 1.75

I. INTRODUCTION

With the increasing demand to know the damping-in-pitch of missiles traveling at supersonic velocities it was decided that instrumentation should be developed for obtaining the data in wind tunnels. Several requirements must be placed upon the apparatus in order to obtain useful data. First, the apparatus should be able to measure small damping moments since the models are small bodies of revolution. Second, the tare damping, i.e., all damping moments except aerodynamic damping, should be as small as possible and repeatable. Third, the model support should not interfere with the flow about the model. Fourth, the apparatus should fit within the test region with little or no modification to the tunnel structure. Fifth, it would be desirable to have oscillating frequencies of the model to be the same as free flight values. Sixth, the center of gravity of the model should be located at the pivot axis. Seventh, it would be desirable to lock or clamp the model to a fixed support during start-up and shut-down of flow in the tunnel. Additional requirements were placed on the instrumentation so that the effect of model center of gravity location and frequency of oscillation on damping could be obtained.

The model chosen for testing was the Army-Navy Spinner Rocket, which is a spin stabilized body of revolution. The wind tunnel model was 5 calibers long (11.25") with a secant ogive nose 2 calibers long (4.50"), a base diameter of 2.25" and a center of gravity location of 4.45" from the model base (Figure 1). It was made of a combination of aluminum and steel parts and had a movable weight located in the nose to position the center of gravity of the model at the prescribed position.

This report presents a description of the apparatus and the technique used to measure the damping-in-pitch on a body of revolution in a supersonic airstream.

II. EXPERIMENTAL PROCEDURE

A. Model Support and Recording System

Several methods of obtaining the damping data were considered and the one that met the prescribed requirements was a system which used a crossed flexure assembly to support the model and to cause it to oscillate about a fixed point. The oscillation was started and the damping-in-pitch was then determined by measuring the rate of subsidence. This system had several distinct advantages which are:

(1) The tare damping, which is due to internal friction of the flexures, was repeatable.

(2) Strain gages mounted on thin flexures were able to measure small loads accurately and reliably if the stresses in the flexures and gages were kept below the yield point of the material.

(3) The flexures provide the restoring moment required to return the model to its initial position.

The system had the disadvantage that the supporting strut, which was made very stiff to insure that the motion was essentially a simple oscillation about a point, limited the length and diameter of the model which could be used.

The original flexure assembly consisted of two sets of flexures, each set containing two flexures mounted 90° to each other with one end of the flexure attached to the model holder and the other end attached to the supporting strut. The thicker flexures, set A of Figure 2, which were the two outer flexures of the assembly, provided the support and restoring force to the model. The thinner flexures, set B, which were located between set A, were used primarily as strain gage mounts. The ends of the flexures were fitted into square keyways and secured to their respective pieces with screws. During the initial tests it was noticed that after the model oscillated several thousands of times the damping rate had changed with no change in test conditions. Upon checking the assembly it was discovered that the flexure ends were not fitting the keyways properly in that only one surface of the flexure

was making metal-to-metal contact with the keyway. Thus the only force to restrain the flexure ends from moving was the frictional force at the surface of the flexure end and the bottom of the keyway and this force was controlled by the tightness of the mounting screws. Since it required checking the unit quite often during a test a redesign of the flexure end connection was made in which the square keyway was changed to a modified "V" groove. This type of end connection required less checking but after several tests were completed the flexure ends would move when the model oscillated. Therefore a new design was developed in which the flexures were made as one unit, eliminating the individual end connections. This unit, shown in Figure 3, was clamped to the strut and model. In addition, the flexures were all made the same thickness. All the test data in this report, however, were taken using the original flexure assembly with the square keyway as shown in Figure 4 (the new flexure unit was not available for these tests).

Strain gages which were mounted on the thinner flexures were used in conjunction with a recording oscillograph and recorded the angle of attack of the model with respect to time. Two strain gages were mounted on each flexure, one on each surface. Figure 5 shows the wiring diagram of the assembly used.

The oscillation of the model was started by a pneumatically operated trigger mounted within the supporting strut (Figure 4). The trigger traveled in an arc, engaged an adjustable horn, rotated the model and then swung past the horn, allowing the model to oscillate. The horn was adjusted to allow the model to trip at a 3.5° angle of attack.

A mechanical locking device was used to prevent overstressing the strain gages and flexures when establishing flow in the test section and to stop the model oscillating if it became unstable. This device was a small cam attached to the supporting strut and operated outside the tunnel with a wire cable. When the cam was rotated it engaged the model, locking it securely to the strut.

The strut assembly was attached to the wind tunnel angle of attack system. The locking cables and air lines were brought out through a side access door of the wind tunnel. Figure 6 shows the photograph of the assembly installed in the wind tunnel.

The model was located in approximately the center of the test section and at a mean angle of attack of zero degrees. It was given an initial angle of attack of 3.5° and then allowed to oscillate about its center of gravity. As the model oscillated a trace showing angle of attack with respect to time was made and simultaneously one-tenth second timing lines were recorded by a recording oscillograph. Figure 7 shows a typical amplitude record made of one test.

The model was tested at various Reynolds numbers over the Mach number range of 1.75 to 4.5. Additional tests were made at several Mach numbers in which most of the boundary layer of the model was made turbulent. This was accomplished by gluing a .20 inch wide sand band on the surface of the nose of the model located 2.25 inches from the nose tip.

B. Reduction of Data and Test Results

The motion of the body may be expressed by the linear differential equation

$$I\ddot{\alpha} + \mu_2 \dot{\alpha} + k_2 \alpha = 0 \qquad (1)$$

where $I\ddot{\alpha}$ is the moment due to the angular acceleration of the body; $\mu_2 \dot{\alpha}$ is the aerodynamic and mechanical damping moment; and $k_2 \alpha$ is the aerodynamic and mechanical restoring moment. Thus μ_2 and k_2 are expressed as

$$\mu_2 = \mu_0 + \mu_1$$

$$k_2 = k_0 + k_1$$

where μ_o and k_0 are the aerodynamic terms and μ_1 and k_1 are the mechanical ones. The solution for equation 1 is

$$\alpha = \alpha_0 e^{-\lambda t}(\cos \omega t + \frac{\lambda}{\omega} \sin \omega t) \qquad (2)$$

where

$$\lambda = \frac{\mu_2}{2I} \text{ and } \omega^2 = \frac{k_2}{I} - (\frac{\mu_2}{2I})^2$$

with the initial conditions of

$$\dot{\alpha} = 0 \ , \ \alpha = \alpha_0 \quad \text{when } t = 0.$$

The equation of the envelope curve or the gradually decreasing amplitude of this damped harmonic motion can be written

$$\alpha = \alpha_0 e^{-\frac{\mu_2 t}{2I}} \tag{3}$$

Thus the total damping term is

$$\mu_2 = \frac{2I}{\Delta t} \log_e \frac{\alpha_0}{\alpha_n} \tag{4}$$

Δt is the time interval between the two model positions of α_0 and α_n .

The maximum amplitudes α_0 , α_1 , α_2 ,.. α_n on the oscillograph records were measured on a Telecordex* machine and the measurements which were in digital form were plotted on semi-logarithmic paper. However, many records were measured with a rule which had one hundred divisions per inch and accurate data were obtained. Figure 8 shows the plot of the record shown in Figure 7. A mean straight line was drawn through the plotted points and the slope of the line was used to determine the decay rate.

The aerodynamic damping coefficient may be determined after correcting for the tare damping. The tare damping was measured by oscillating the model on the same support system in the tunnel with no flow and at various pressures from 76 to 3.5 cm mercury absolute and recording the motion on the oscillograph. The curve of the damping term μ_1 versus tunnel pressure was extrapolated to zero pressure to obtain the tare damping. Since the tare damping varied with model oscillatory frequency, data were obtained by changing the moment of inertia of the model and the results are shown in Figure 9. Also it was noticed that tare damping varied with amplitude and therefore to minimize this effect data were obtained in the 2.25° to 1.75° amplitude range for all tests including "flow-on" and "flow-off".

---

* The Telecordex machine is a two channel indicating and recording instrument and is capable of measuring the amplitude of each oscillation and presenting this measurement in recorded digital form.

With the tare damping moment known the aerodynamic damping moment may be obtained. The equation is

$$\mu_0\dot{\alpha} = \mu_2\dot{\alpha} - \mu_1\dot{\alpha} .$$

The damping coefficient is defined as

$$K_H = \frac{\mu_0}{\rho d^4 u} . \qquad (5)$$

The coefficient K_H versus Mach number for the model is shown in Figure 10. Included on the graph are the results of the free flight range data[1] and a theoretical estimate using the Zero Order Theory[2] (presented in the appendix).

Several tests were made at Mach numbers 3.0, 4.0, and 4.50 in which the Reynolds number was varied. The results are presented in Table I. As can be seen there was an indication of increase of damping with increase of Reynolds number. However, the total spread of the data was within the experimental accuracy.

Additional tests were made in which a sand band was placed on the nose of the model to cause the boundary layer to become turbulent. The difference in damping rates between the tests with and without transition band in three out of four tests was less than 4 per cent which is well within the experimental accuracy of the data (refer to Table I and Figure 10). Figures 11 and 12 are shadowgraph photos which show the type of boundary layer on the model at the various test conditions. Schlieren pictures were also taken to show the general flow over the model (Figure 13).

The test program was started in tunnel No. 3 and considerable difficulty in measuring th damping rates in the low Mach number range was encountered. At Mach number 1.73 model oscillations were induced by unsteadiness in the flow, making it impossible to obtain reliable data. A record of such a test is presented in Figure 14 showing the motion of the model before and after it was tripped. As a comparison Figure 15 shows the motion of the model when tested in tunnel No. 1 at Mach number 1.75 with same test conditions.

The accuracy of the data depends upon the amplitude records, moment of inertia, and the stagnation pressure of the wind tunnel. The envelope of an amplitude record was measured several times by three individuals and the maximum difference in μ_2 was 4 percent. The moment of inertia of the model was measured on a torsional pendulum spring electronic instrument with an accuracy of 2 percent. The tunnel stagnation pressure was measured to within $\pm$ 2 mm of Mercury absolute of set pressure.

C. Wind Tunnel

The tests were conducted in the Ballistic Research Laboratories' Flexible Nozzle Tunnels No. 1 and 3. They are continuous operation, closed circuit, variable density supersonic wind tunnels with a Mach number range of 1.25 to 5.00. The test section dimensions of No. 1 tunnel are 15 inches high and 13 inches wide, for No. 3 tunnel are 13 inches high and 15 inches wide for Mach numbers of 2.00 to 5.00 and 20 inches high and 15 inches wide for Mach numbers of 1.25 to 2.00. The top and bottom walls of the test sections are sloped to account for the boundary layer growth on the walls. The Mach number distribution along the centerline for tunnel No. 1 are within $\pm$ .008 of mean Mach number and the flow inclination is within $\pm$ .1°. For tunnel No. 3 the Mach number distributions are within $\pm$ .030 and the flow inclination is within $\pm$ .5°. A schlieren optical system and a spark shadowgraph unit are used to make visual observations of the flow about the model.

III. CONCLUSIONS

1. All parts of the model which are to be used as a fixed unit should be locked tight in order to prevent any secondary motion.

2. The mounting strut should be stiff and tight so that the motion is essentially a simple oscillation about the cross points of the flexures.

3. The wind tunnel flow must be reasonably steady so that model oscillations are not induced by the unsteadiness in the flow.

4. The damping coefficient is a function of Mach number and decreases with increasing Mach number for the model tested.

5. The damping coefficient is not very sensitive to changes in Reynolds number or whether the boundary layer of the model is laminar or turbulent.

6. Reasonable comparisons with range data were made.

H. E. MALOY, JR.

IV. APPENDIX

As far as the author knows no exact theory exists that predicts the damping-in-pitch of bodies of revolution traveling at supersonic velocities. A theory referred to as the Zero Order Theory was developed by M. Munk (Ref. 2). The following is the development of this theory:

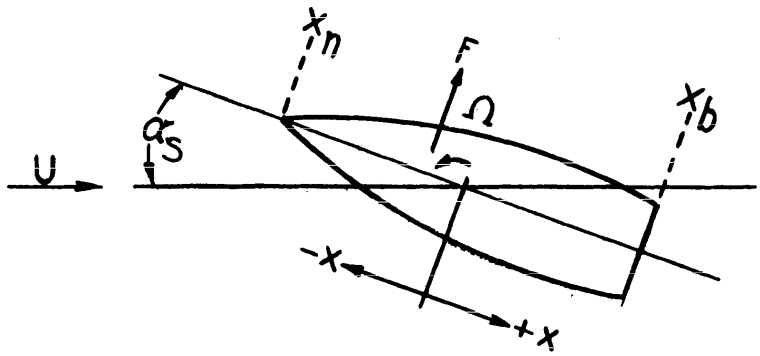

The force per unit length normal to the x-axis at any given x is

$$F_x = \frac{\partial F}{\partial x} = \frac{d}{dt}(\rho u S) \tag{6}$$

where $u = \Omega x + U \sin \alpha_s$ (7)

S is cross sectional area of model

Since α is small Eq. 7 may be written

$$\frac{u}{U} = \frac{\Omega x}{U} + \alpha_s$$

Let $\alpha_s = A \cos \omega t$

$$\dot{\alpha} = \dot{\alpha}_s = -A\,\omega \sin \omega t \text{ and } \alpha_\omega = -A\,\omega \frac{x}{U} \sin \omega t$$

$$F_x = \rho U \frac{d}{dt}\left[\left(A \cos \omega t - A\,\omega \sin \omega t \frac{x}{U} \right) S\right] \tag{8}$$

Now

$$\frac{d}{dt} = \frac{\partial}{\partial t} + \frac{\partial}{\partial x}\frac{dx}{dt} = \frac{\partial}{\partial t} + u \frac{\partial}{\partial x}$$

Then equation 8 becomes

$$F_x = \rho U \left[S\left(\frac{\partial \alpha_s}{\partial t} + \frac{\partial \alpha_\omega}{\partial t}\right)\right] + \rho U^2 \left[(\alpha_s + \alpha_\omega)\frac{\partial s}{\partial x} + S \frac{\partial}{\partial x}(\alpha_s + \alpha_\omega)\right]$$

The moment equation is

$$M_x = F_x \cdot x \tag{9}$$

Substituting for $\frac{\partial \alpha_s}{\partial t}$, $\frac{\partial \alpha_\omega}{\partial t}$ and F_x and integrating over the entire length of the body

$$M = 2 \rho U \int_{=n}^{b} xS A \omega \sin \omega t \, dx - I_{cg} A \omega^2 \cos \omega t$$

$$+ \rho U^2 A \cos \omega t \left[x_b S_b - \text{vol} \right]$$

$$- \rho U \omega A \sin \omega t \left[x_b^2 S_b \right] - 2 \int_{x_n}^{x_b} S x \, dx \tag{10}$$

Let $\delta = A \cos \omega t$

$$\dot{\delta} = \omega A \sin \omega t$$

$$\ddot{\delta} = -\omega^2 A \cos \omega t$$

Then equation (10) becomes

$$M = I_{cg} \ddot{\delta} + \rho U x_b^2 S_b \dot{\delta} + \rho U^2 \left[x_b S_b - \text{vol} \right] \delta \tag{11}$$

Consider the $\dot{\delta}$ term which is the damping moment of equation (11) and let

$$\mu_o = \rho U x_b^2 S_b \tag{12}$$

Putting equation (12) in coefficient form

$$K_H = \frac{\mu_o}{\rho U d^4} = \frac{x_b^2 S_b}{d^4}$$

where x_b = distance from base to cg

S_b = cross-section area of base

Thus for the model tested

$$K_H = 3.07$$

V. REFERENCES

1. Murphy, C. H., Schmidt, L. E., -- "The Effect of Length on the Aerodynamic Characteristics of Bodies of Revolution in Supersonic Flight", BRL Report 876.

2. Munk, Max M., "The Aerodynamic Forces of Airship Hulls", NACA Report 184.

TABLE I

A. N. SPINNER ROCKET MODEL

Test No.	Ma. No.	P_0*	Sand Band	Freq. Cycles/sec	Re	K_H
102,103	4.50	350	No	11.48	9.47×10^5	3.34
106,107	4.50	250	No	10.79	6.76×10^5	3.36
910,911	4.00	329	No	9.56	10.91×10^5	3.91
908,909	4.00	250	No	10.52	8.30×10^5	3.80
942,943	4.00	250	Yes	10.45	8.30×10^5	3.66
939,941	4.00	140	Yes	11.66	4.66×10^5	3.83
907	4.00	140	No	11.67	4.66×10^5	3.39
034,035	3.00	175	No	8.18	9.30×10^5	4.24
952,953	3.00	175	Yes	8.18	9.30×10^5	4.19
954,955	3.00	100	Yes	10.47	5.30×10^5	4.11
038,039	3.00	100	No	10.63	5.30×10^5	4.08
925,926	2.50	79.9	No	10.00	5.60×10^5	4.37
933,934	1.75	80	No	6.36	7.94×10^5	5.23

* (Cm. Hq. Abs.)

Re based on Model Diameter of 2.25"

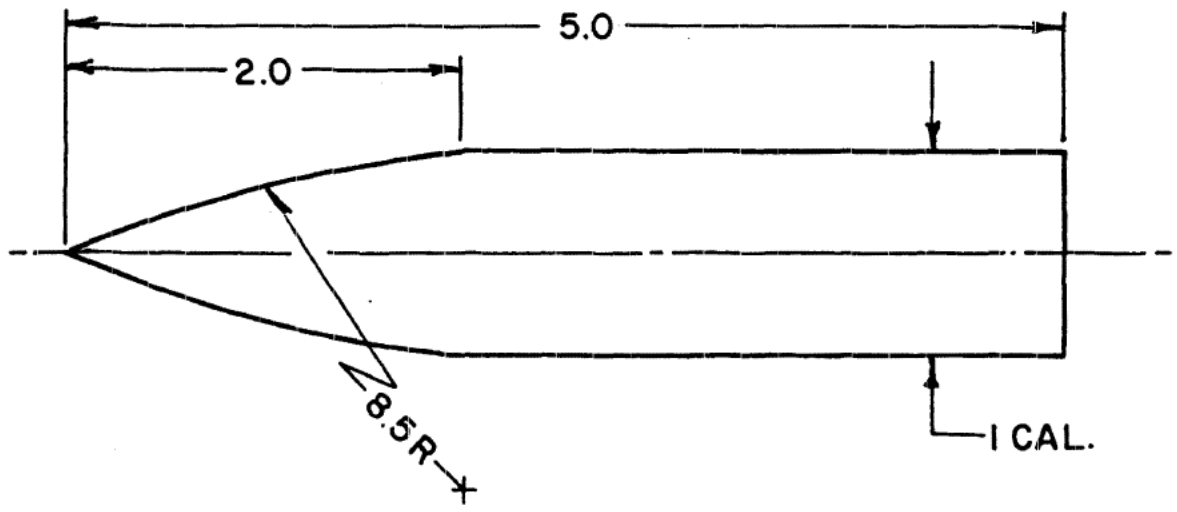

FIG. 1

NOTE:
ALL DIMENSIONS IN CALIBERS
1 CALIBERS = 2.250 INCHES

FIG. 1

5 CALIBER
OGIVE CYLINDER

SUPERSONIC WIND TUNNELS, LAB.
BALLISTIC RESEARCH LAB, A.P.G, MD

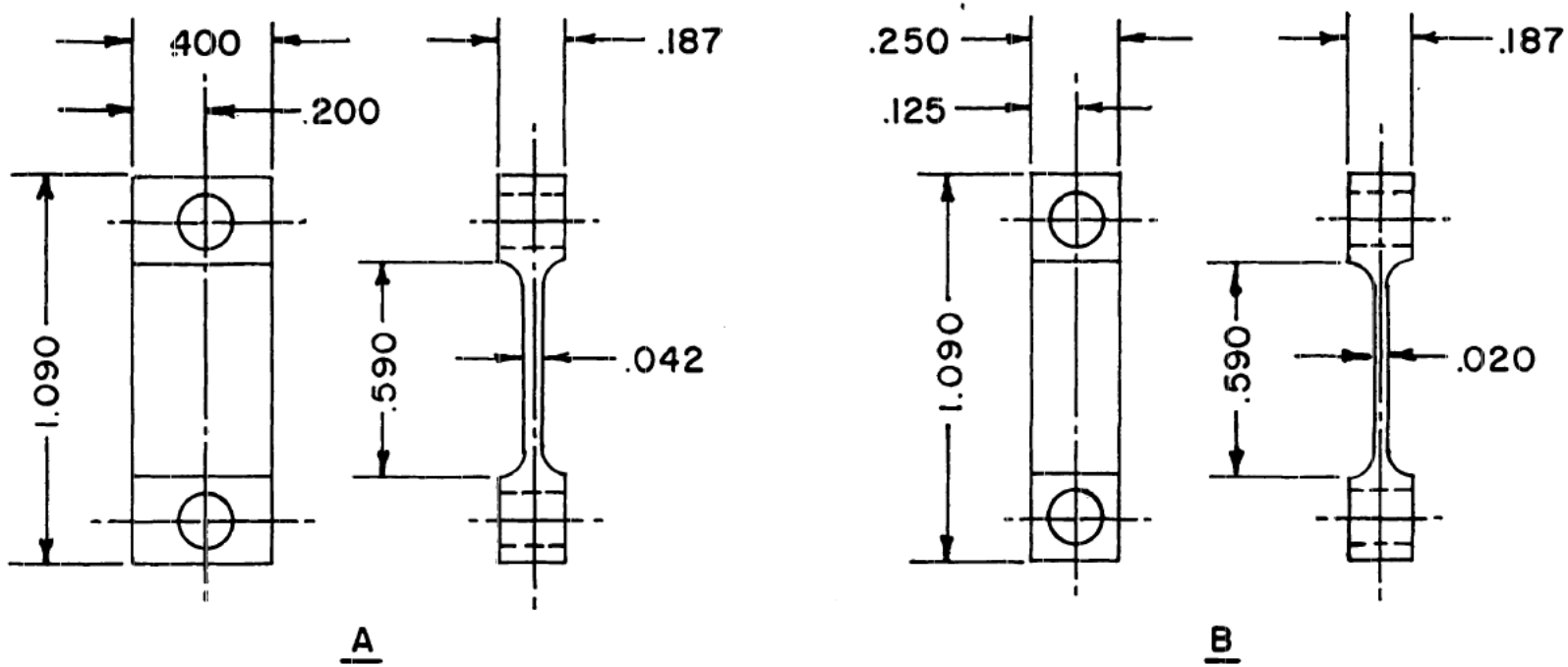

NOTE:
ALL DIMENSIONS IN INCHES

FIG. 2

FLEXURES
JAN SPINNER ROCKET

SUPERSONIC WIND TUNNELS LAB.
BALLISTIC RESEARCH LAB. A.P.G. MD.

FIG. 2

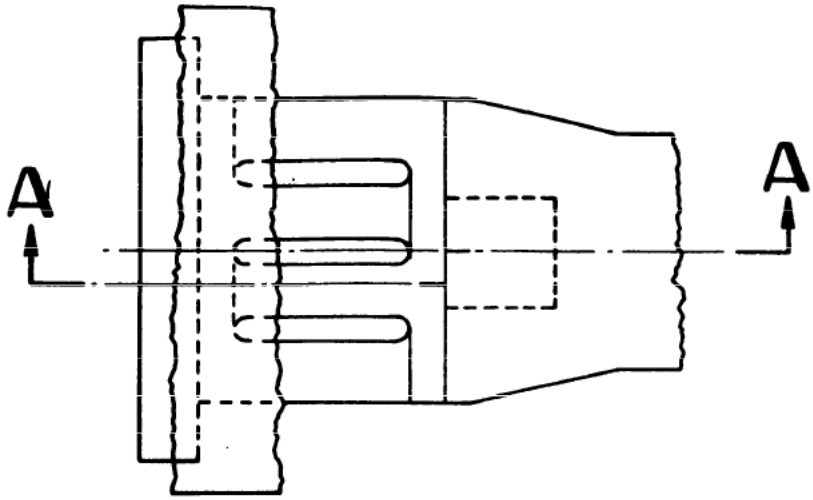

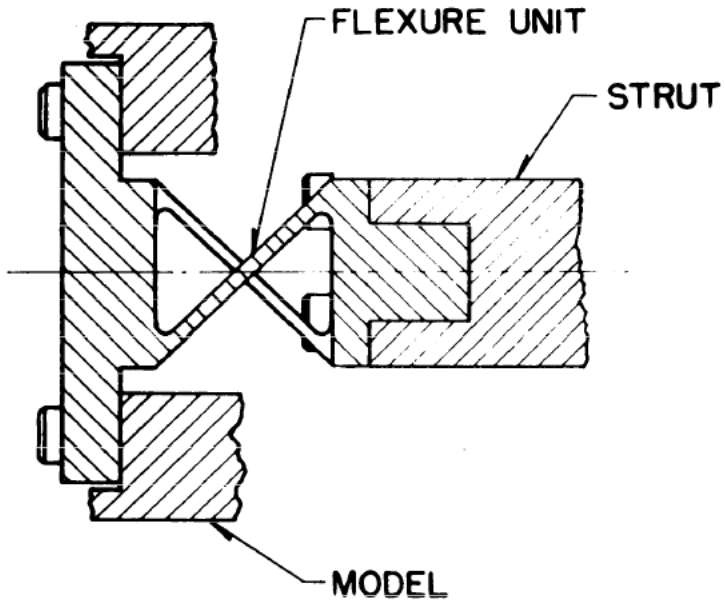

SECTION A-A

FLEXURE UNIT ASSEMBLY
DYNAMIC STABILITY

FIG.3	SUPERSONIC WIND TUNNELS LAB. BALLISTIC RESEARCH LAB., A.P.G., MD.	FEB. 1958

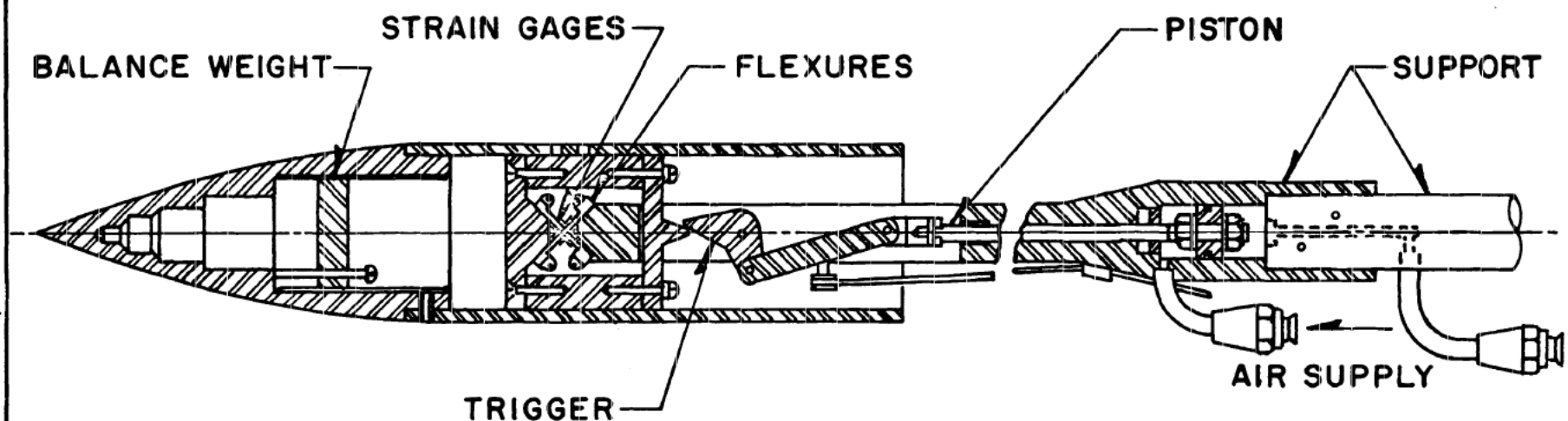

FIG. 4

MODEL SUPPORT SYSTEM
DYNAMIC STABILITY

SUPERSONIC WIND TUNNELS LAB
BALLISTIC RESEARCH LAB. A.P.G. MD

FIG. 4

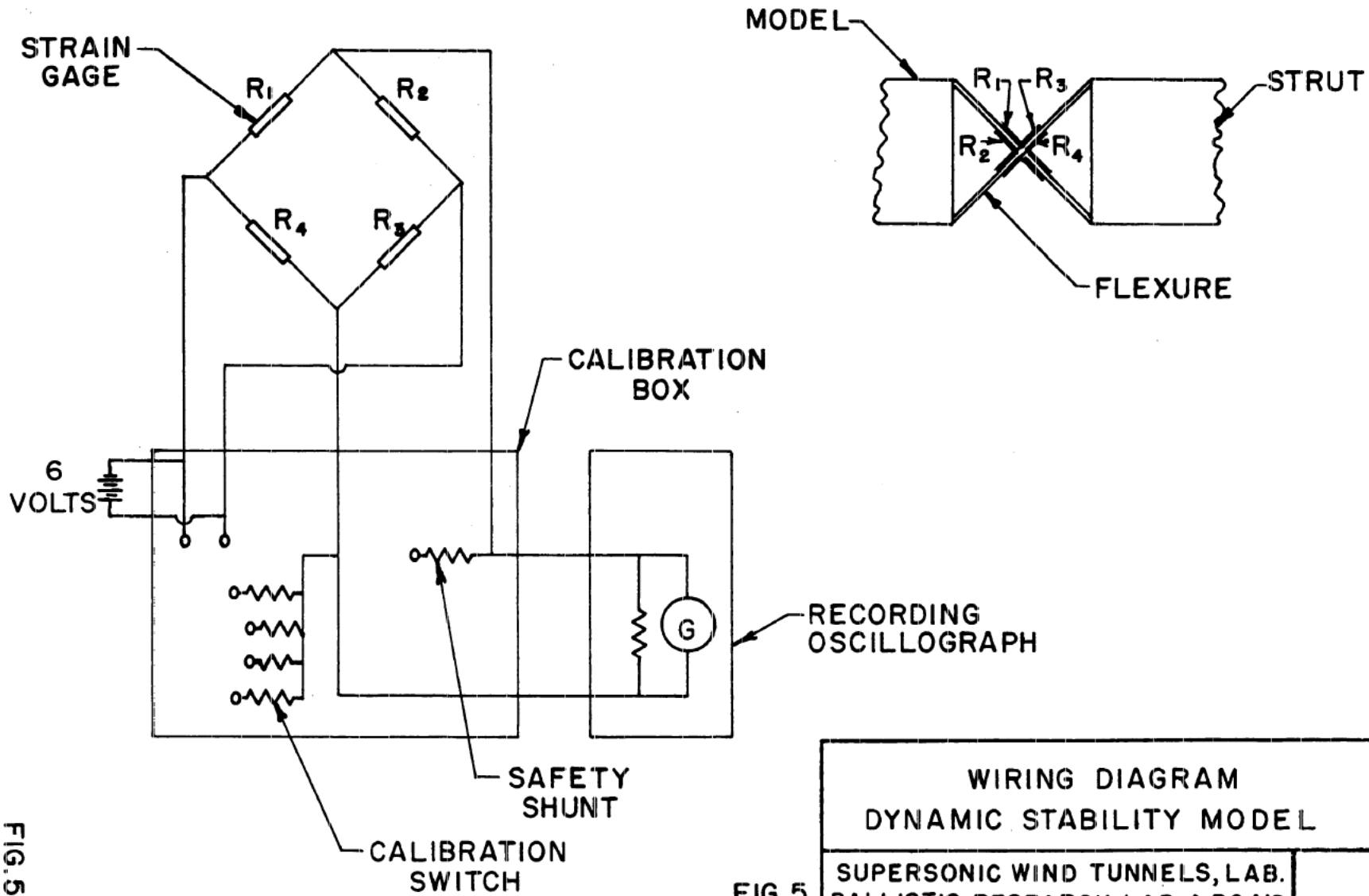

FIG. 5

WIRING DIAGRAM
DYNAMIC STABILITY MODEL

SUPERSONIC WIND TUNNELS, LAB.
BALLISTIC RESEARCH LAB, A.P.G. MD.

FIG. 5

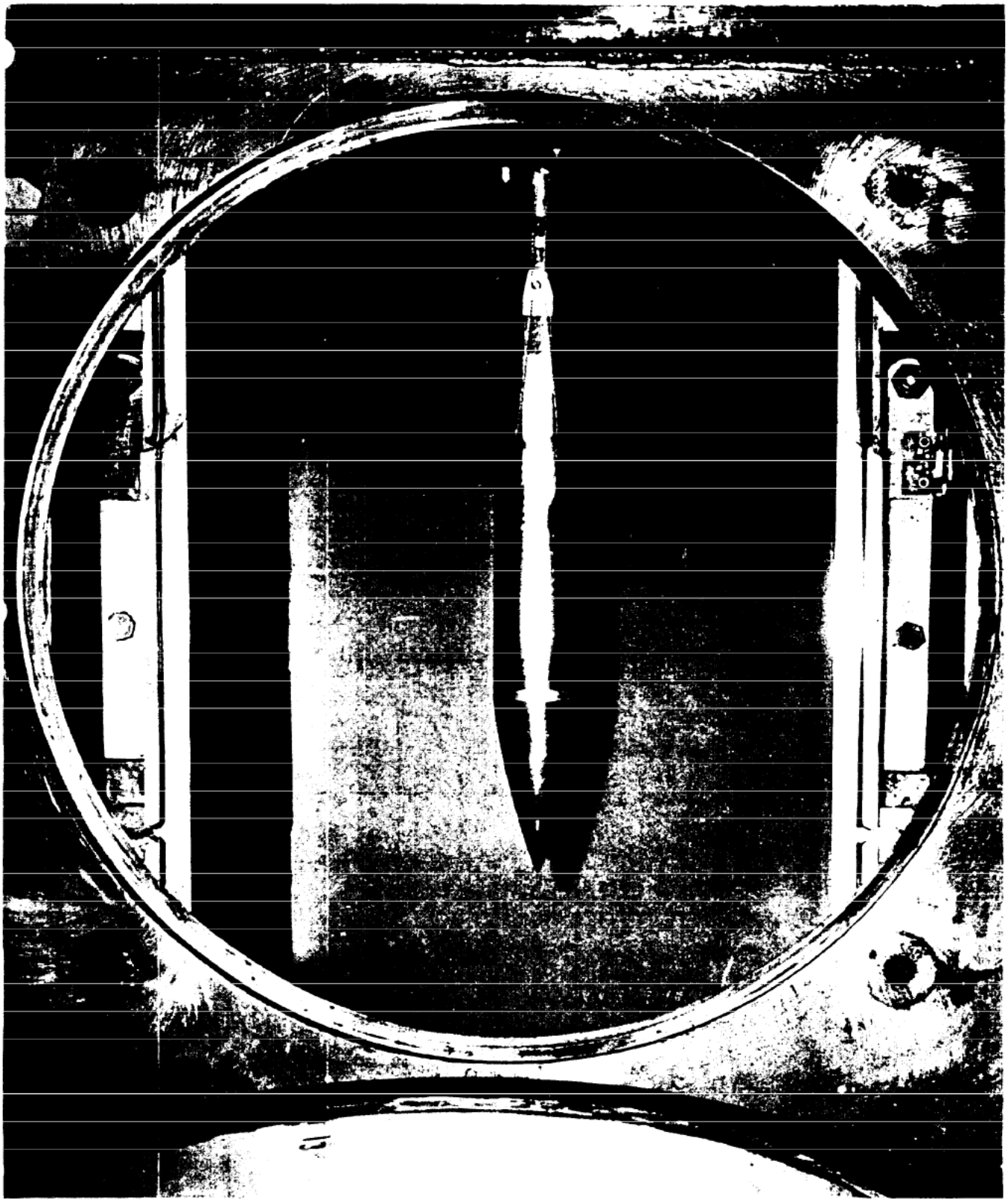

Fig. 6 Photograph of model installed in tunnel.

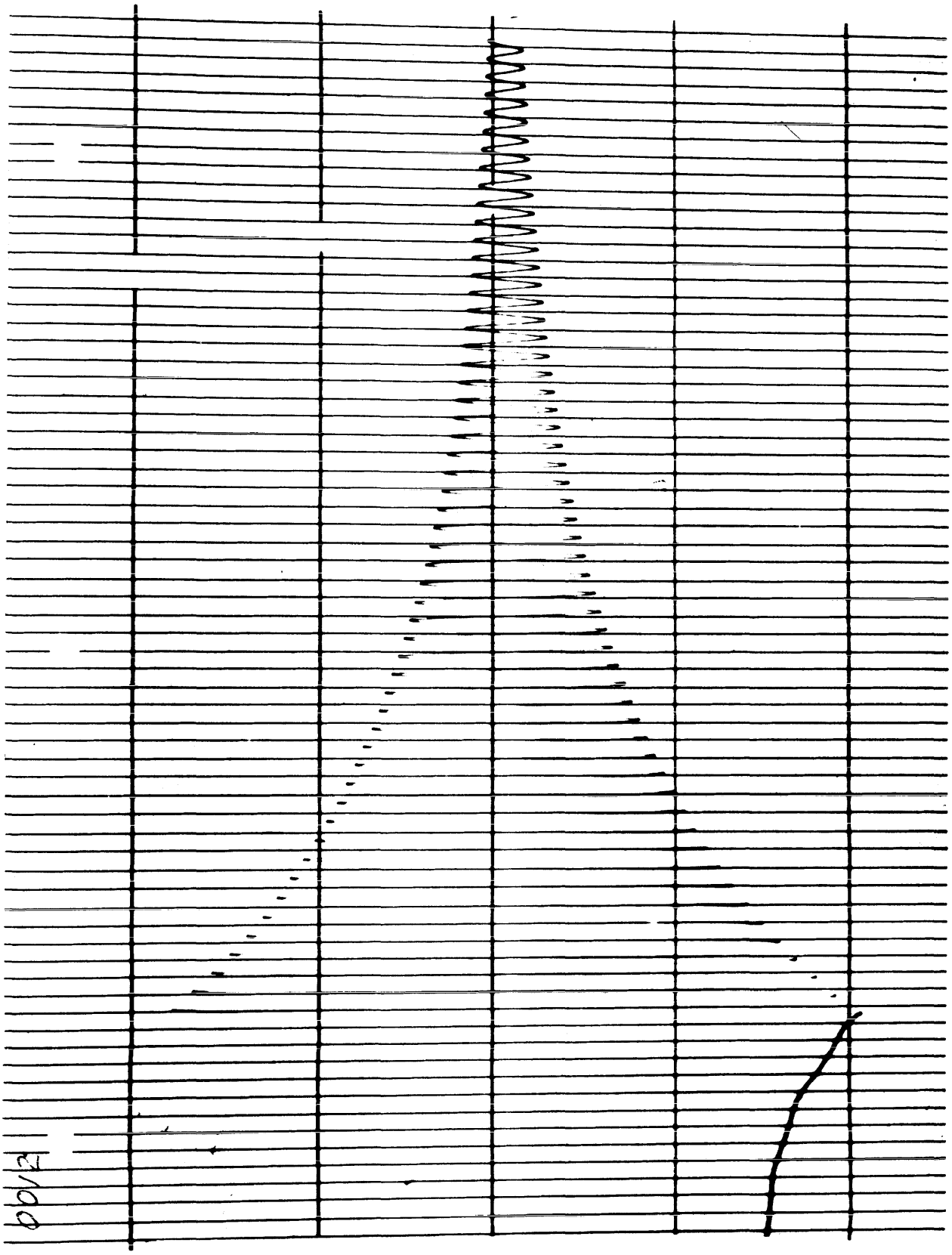

Fig. 7 Reproduction of typical oscillograph record.

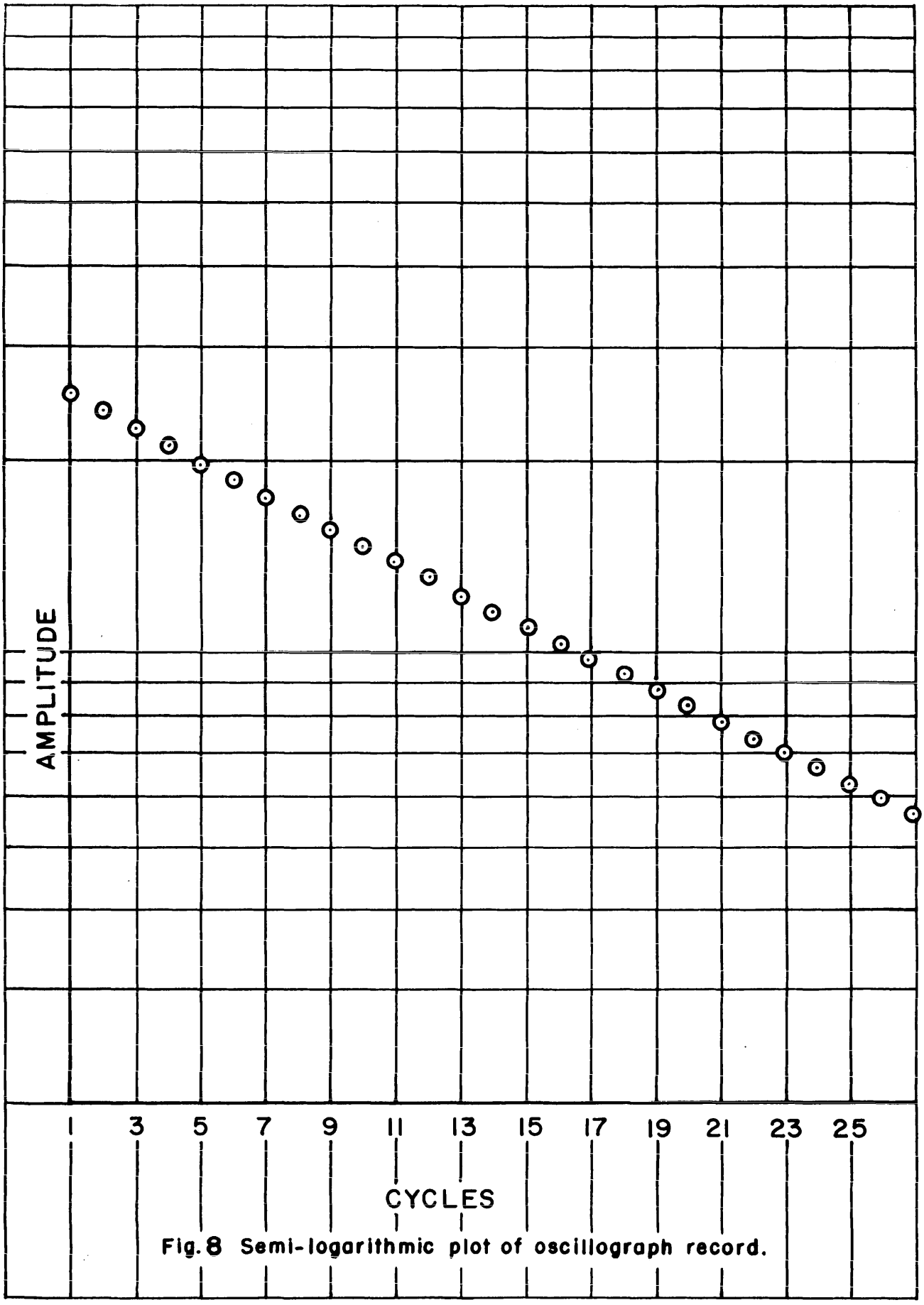

Fig. 8 Semi-logarithmic plot of oscillograph record.

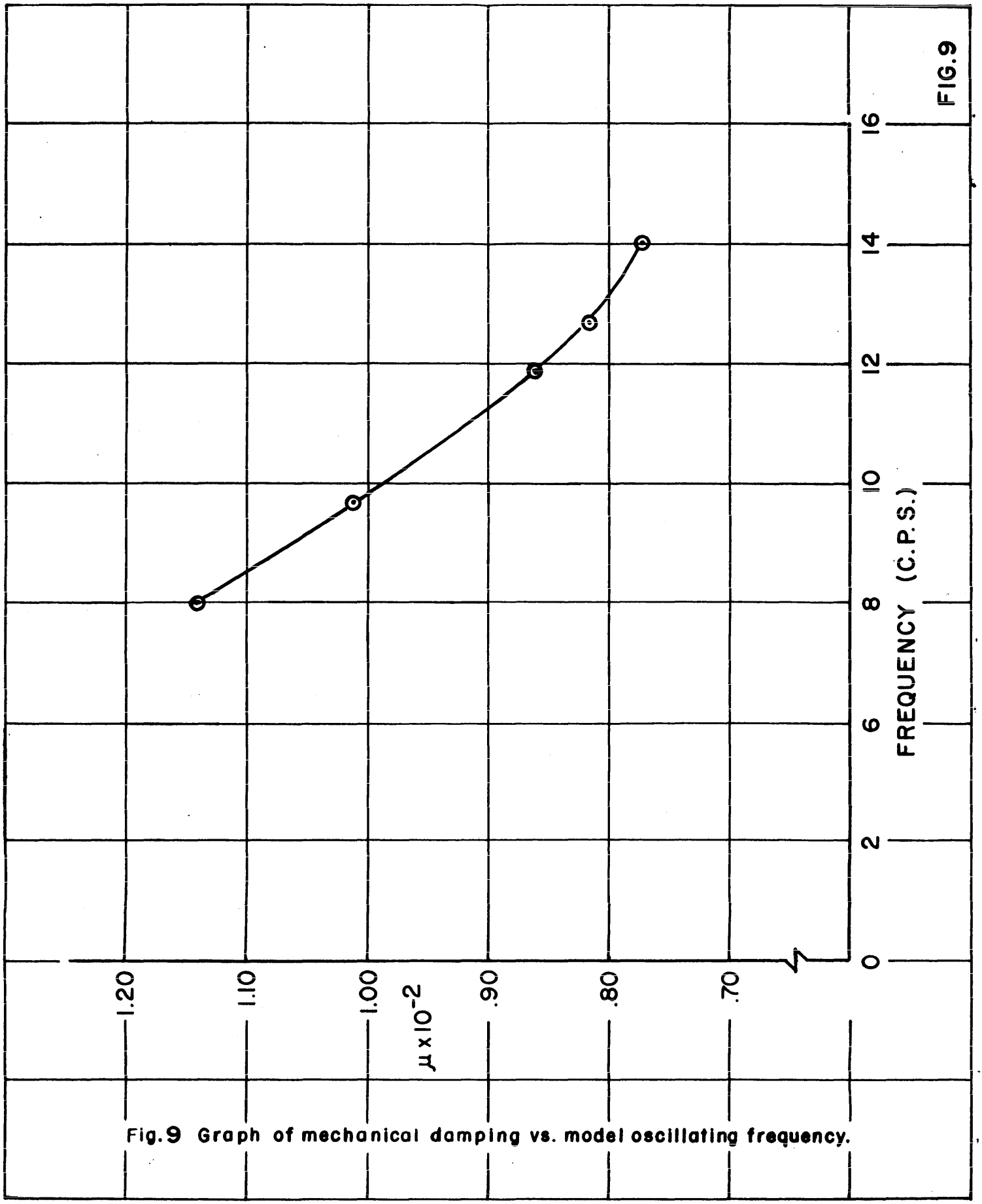

Fig.9 Graph of mechanical damping vs. model oscillating frequency.

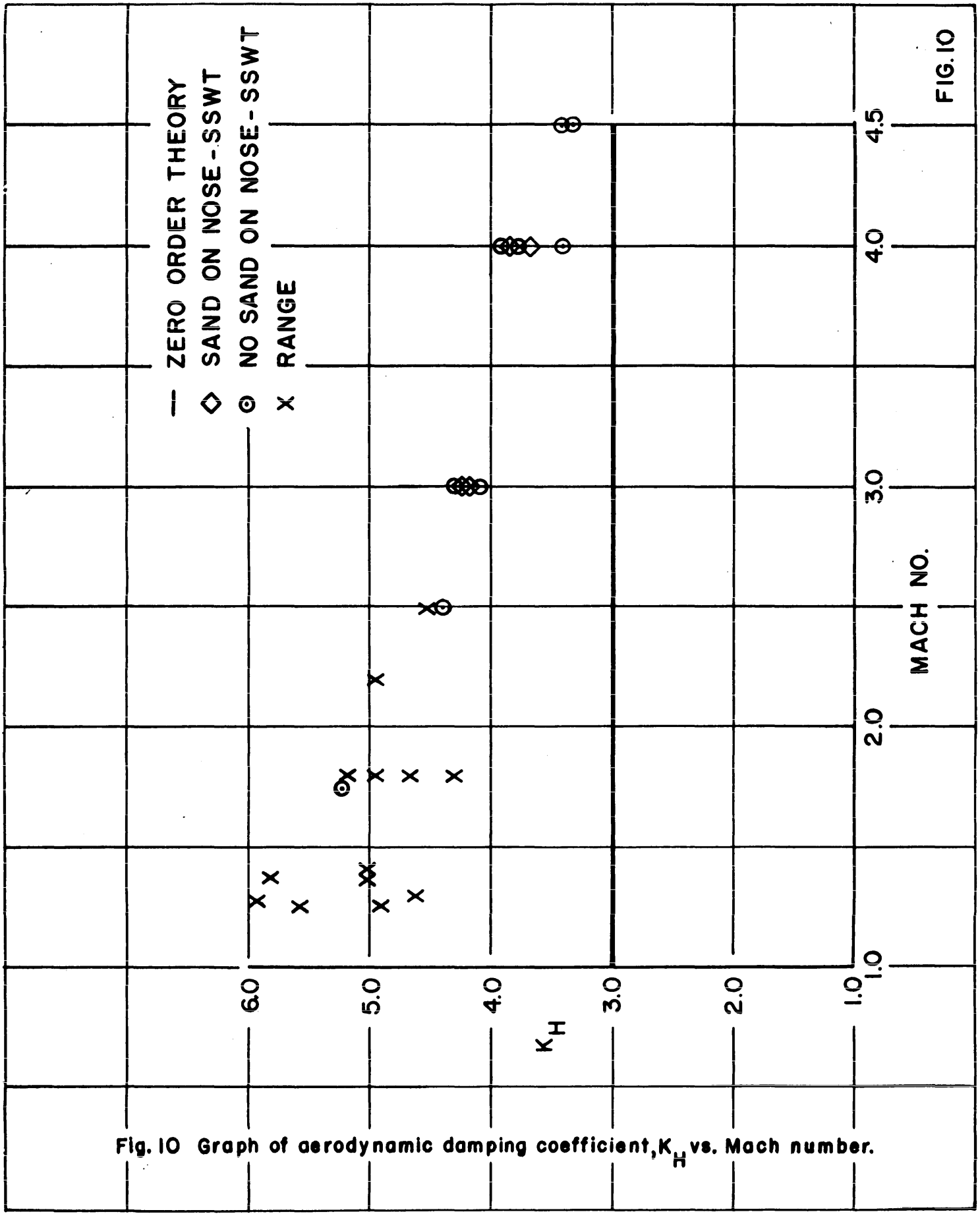

Fig. 10 Graph of aerodynamic damping coefficient, K_H vs. Mach number.

MACH NO. = 3.00 α = 0°
WITHOUT SANDBAND

MACH NO. = 3.00 α = 0°
WITH SANDBAND

FIG. 11

MACH NO. = 3.00 $\alpha = 2°$
WITHOUT SANDBAND

MACH NO. = 3.00 $\alpha = 2°$
WITH SANDBAND

FIG. 12

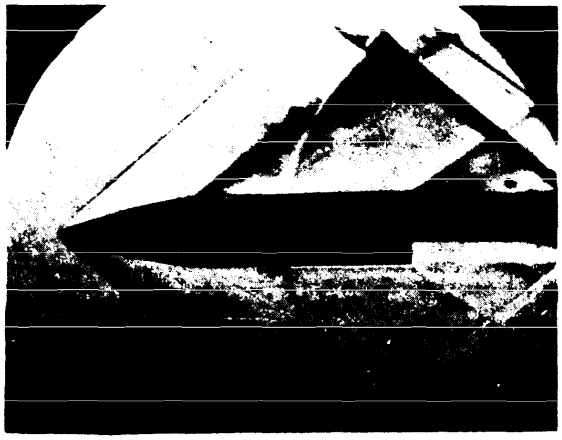

MACH NO. = 1.75

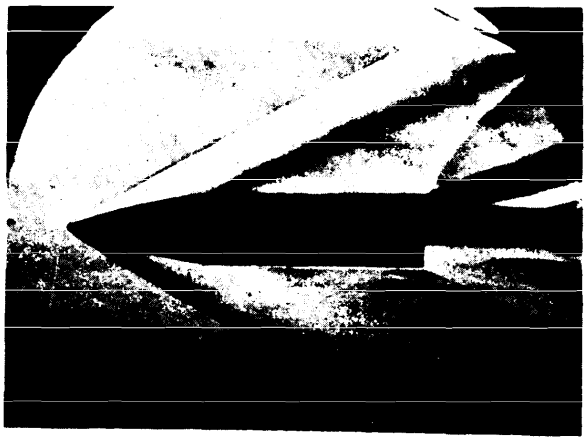

MACH NO. = 2.50

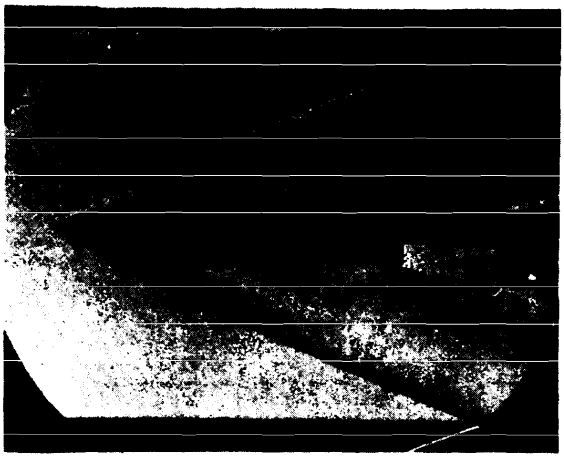

MACH NO. = 3.00

MACH NO. = 4.00

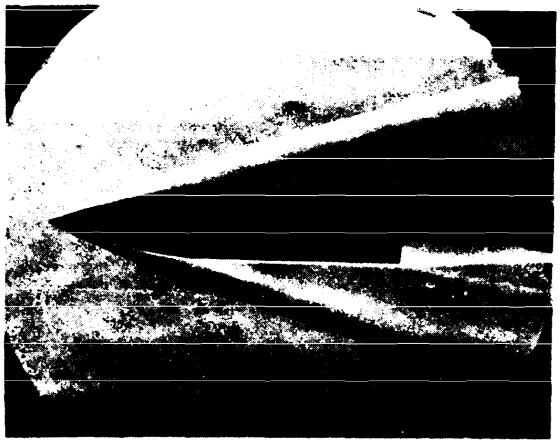

MACH NO. = 4.50

FIG. 13

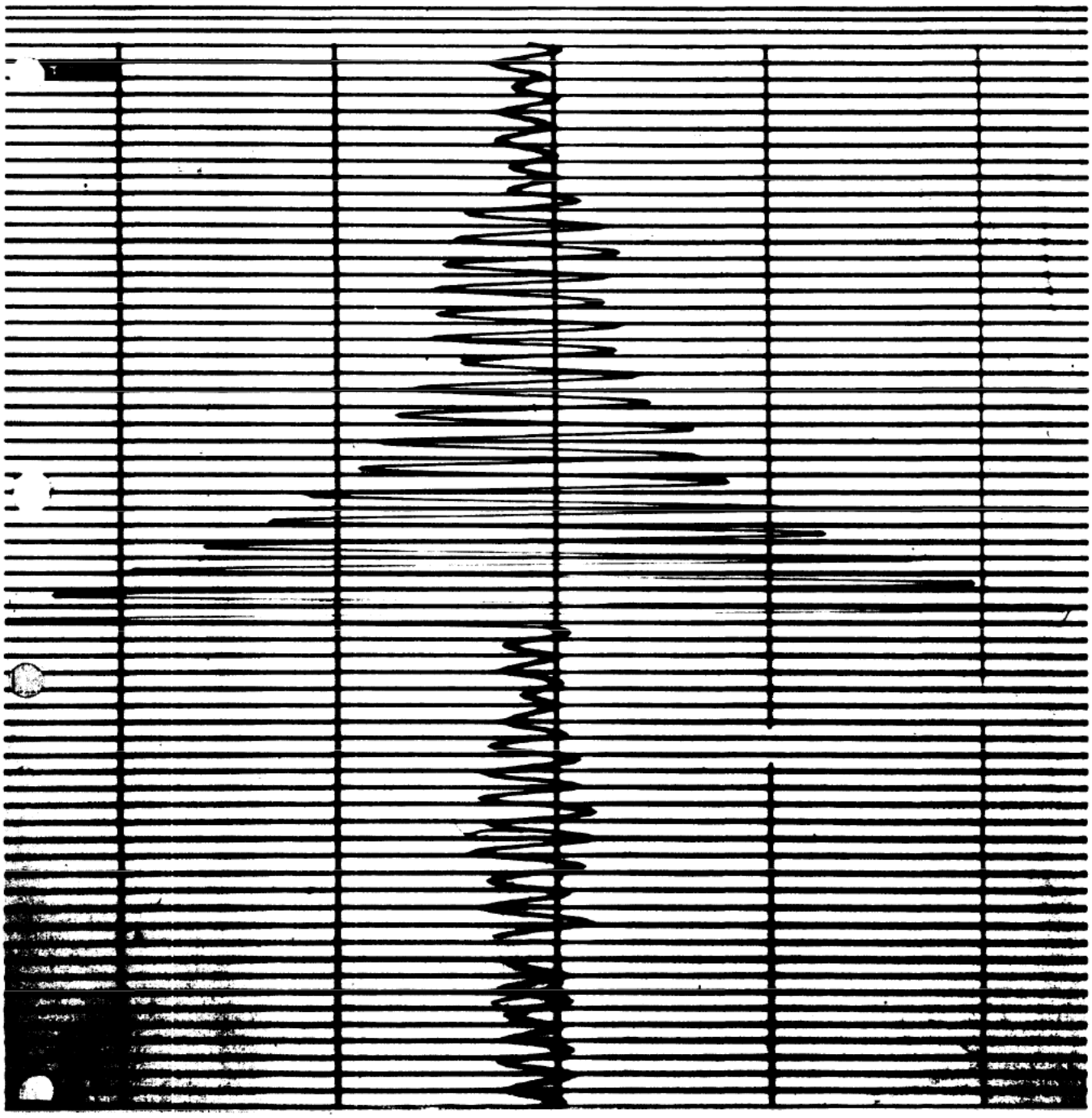

Fig.14 Reproduction of an oscillograph record showing flow disturbance in tunnel No. 3 at Mach 1.73 .

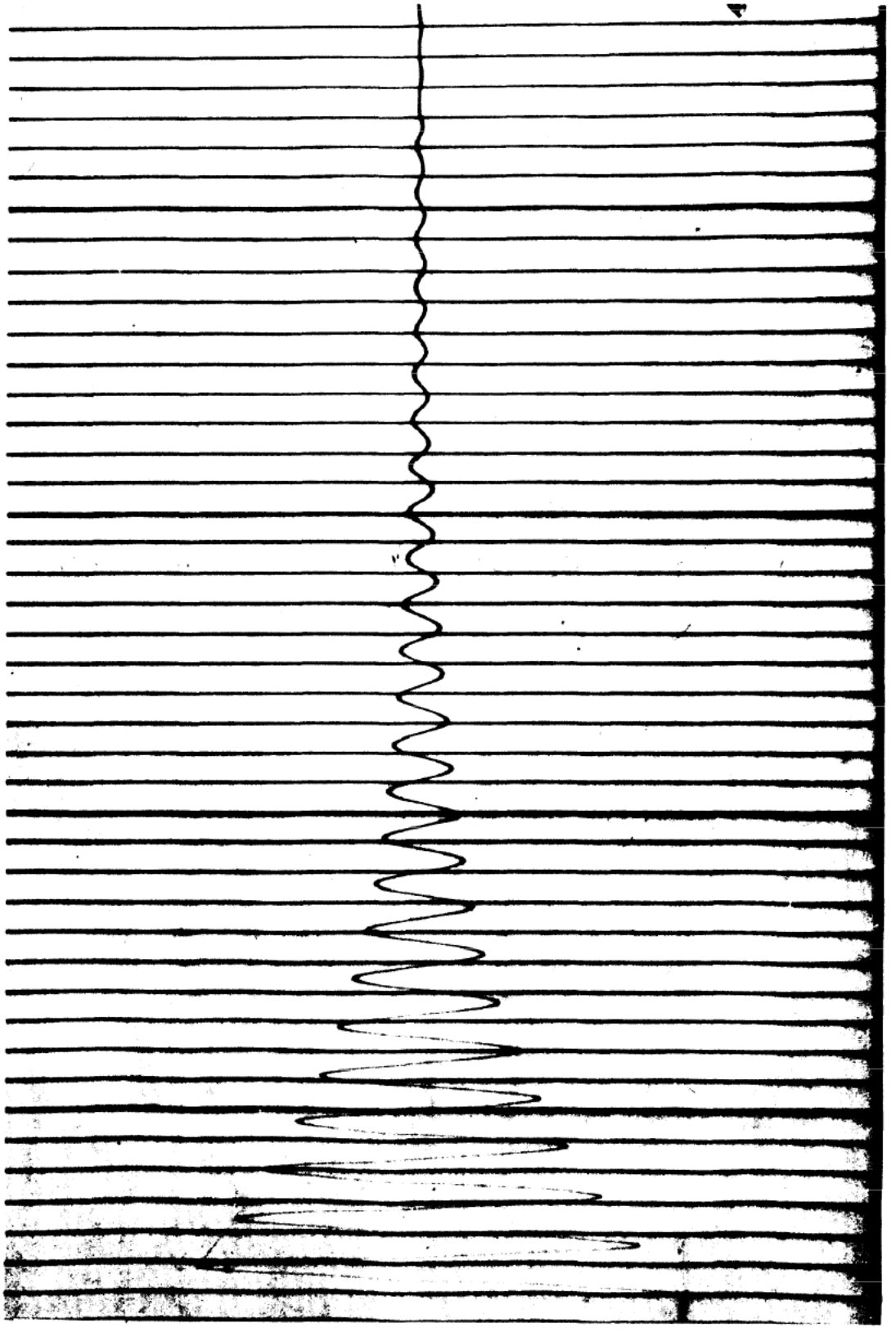

Fig.15 Reproduction of an oscillograph record showing absence of flow disturbance in tunnel No. 1 at Mach 1.75 .

DISTRIBUTION LIST

No. of Copies	Organization
1	Chief of Ordnance Department of the Army Washington 25, D. C. Attn: ORDTB - Bal Sec
1	Commanding Officer Diamond Ordnance Fuze Laboratories Washington 25, D. C. Attn: ORDTL - 012
10	British Joint Services Mission 1800 K Street, N. W. Washington 6, D. C. Attn: Reports Officer
4	Canadian Army Staff 2450 Massachusetts Avenue Washington 8, D. C. Of Interest To: Dr. G. V. Bull, CARDE
1	Commander U. S. Naval Ordnance Test Station China Lake, California Attn: Dr. H. R. Kelly
2	Commander Naval Ordnance Laboratory White Oak Silver Spring, Maryland Attn: Dr. Kurzweg Dr. E. Krahn
1	Naval Supersonic Laboratory Massachusetts Institute of Technology Cambridge 39, Massachusetts Attn: Mr. Grank H. Durgin
2	Commander Air Proving Ground Center Eglin Air Force Base, Florida Attn: Dr. Alan Galbraith Mr. Foster Burgess
3	Director National Aerouautics and Space Agency Langley Field, Virginia Attn: Mr. J. Bird Mr. C. E. Brown Dr. A. Buseman
1	Director National Aeronautics and Space Agency Lewis Flight Propulsion Laboratory Cleveland Airport Cleveland, Ohio Attn: Dr. Evaard
3	Director National Aeronautics and Space Agency Ames Laboratory Moffett Field, California Attn: Dr. A. C. Charters Mr. H. J. Allen
1	Director National Bureau of Standards Connecticut Ave. & Van Ness Sts, N. W. Washington 25, D. C. Attn: Mr. G. B. Schubauer
10	Commanding Officer Office of Ordnance Research Box CM, Duke Station Durham, North Carolina
1	Jet Propulsion Laboratory 4800 Oak Grove Drive Pasadena 2, California Attn: Dr. F. Goddard

DISTRIBUTION LIST

No. Of Copies	Organization
1	Aero Physics Development Corporation P. O. Box 657 Pacific Palisades, California Attn: Dr. William Bollay
1	The Eglin Corporation 2925 Merrill Road P. O. Box 13214 Dallas 20, Texas Attn: Dr. Floyd L. Cash
1	Cornell University Graduate School of Aeronautical Engineering Ithaca, New York Attn: Dr. W. R. Sears
2	Princeton University Aeronautics Department Forrestal Research Center Princeton, New Jersey Attn: Prof. S. Bogdonoff Prof. W. Hayes
1	University of Texas Defense Research Laboratory 500 East 24th Street Austin, Texas Attn: Mr. J. B. Oliphint
1	Guggenheim Aeronautical Laboratory California Institure of Technology Pasadena 4, California Attn: Prof. H. W. Liepman
1	Dr. R. Bolz Case Institute of Technology Cleveland, Ohio

No. of Copies	Organization
1	Professor Francis H. Clauser Chairman, Department of Aeronautics Johns Hopkins University Baltimore 18, Maryland
1	Professor G. Carrier Division of Applied Sciences Harvard University Cambridge 38, Massachusetts
1	Professor H. W. Emmons Harvard University Cambridge, Massachusetts
1	Professor C. B. Millikan Guggenheim Aeronautical Laboratory California Institute of Technology Pasadena 4, California

DISTRIBUTION LIST

ABSTRACT CARDS ONLY

No. Of Copies	Organization
1	Allegany Ballistic Laboratory Cumberland, Maryland
1	AVCO Manufacturing Corporation Research and Development Division 201 Lowell Street Wilmington, Massachusetts
2	Budd Company Red Lion Plant Philadelphia 15, Pennsylvania Attn: Mr. C. B. Wileman, Weapons Div. Mr. A. F. Stranges, Weapons Div.
1	Capehart-Farnsworth Corporation Fort Wayne, Indiana Attn: Mrs. Margaret Moyer
1	Chamberlain Corporation Waterloo, Iowa Attn: Mr. Irving Herman
1	Douglas Aircraft Company Santa Monica, California Attn: Mr. W. S. Cohen
1	General Electric Company Research Laboratory Schenectady, New York Attn: Library
1	Grumman Aircraft Engineering Corporation Bethpage, New York Attn: Mr C. Tilgner, Jr.
1	North American Aviation, Inc. Aeronuatical Laboratory Downey, California Attn: Dr. E. R. Nan Driest
1	Ramo-Wooldridge Corporation 409 East Manshester Blvd. Inglewood, California Attn: Dr. Louis G. Dunn
1	United Aircraft Corporation East Hartford, Connecticut Attn: Mr. M. Schweiger
2	Brown University Graduate Division of Applied Mathematics Providence 12, Rhode Island Attn: Dr. R. Probstein Prof. W. Prager
1	University of California at Los Angeles Department of Engineering Los Angles 25, California Attn: Dr. L. M. Boelter
1	Case Institute of Technology Cleveland, Ohio Attn: Dr. G. Kuerti
1	Catholic University of America Department of Physics Washington 17, D. C. Attn: Prof. K. F. Herzfeld Prof. M. Monk
1	Cornell Aeronautical Laboratory Buffalo, New York Attn: Dr. A. Flaz Dr. Ira G. Ross
1	Space Technology Laboratory 5730 Arbor Vistae Street Los Angeles, California Attn: Dr. Louis G. Dunn

DISTRIBUTION LIST

ABSTRACT CARDS ONLY

No. of Copies	Organization
1	Harvard University Department of Applied Physics & Engineering Science Cambridge 38, Massachusetts Attn: Dr. A. Bryson
1	Johns Hopkins University Department of Mechanical Engineering Baltimore 18, Maryland Attn: Dr. S. Corrsin
1	The Johns Hopkins University Department of Aeronautical Engineering Baltimore 18, Maryland Attn: Dr. L. Kovasznay
1	Lehigh University Physics department Bethlehem, Pennsylvania Attn: Dr. R. Emrich
1	Lockheed Missile Systems Division Box 504 Sunnyvale, California Attn: Mr. R. Smelt
1	University of Maryland Institute of Fluid Dynamics & Applied Mathematics College Park, Maryland Attn: Director
1	University of Maryland Department of Aeronautical Engineering College Park, Maryland Attn: Dr. F. Shen
1	Massachusetts Institute of Technology Department of Aeronautical Engineering Cambridge 39, Massachusetts Attn: Prof. J. R. Markham
1	The Martin Company Baltimore 3, Maryland Attn: Dr. V. Morkonin Chief, Aerophysics Research Flight Vehicle Design Department
1	University of Michigan Department of Aeronautical Engineering East Engineering Building Ann Arbor, Michigan Attn: Dr. Arnold Kuethe
1	University of Minesota Department of Aeronautical Engineering Minneapolis 14, Minnesota Attn: Dr. R. Hermann
1	University of Minesota Department of Mechanical Engineering Division of Thermodynamics Minneapolis, Minnesota Attn: Dr. E. R. G. Eckert
1	National Science Foundation Washington 25, D. C. Attn: Dr. R. Seeger
1	New York University Department of Aeronautics University Heights New York 53, New York Attn: Dr. J. F. Ludloff
1	New York University Institute of Mathematics & Mechanics 45 Fourth Street New York 53, New York Attn: Dr. R. W. Courant

DISTRIBUTION LIST

ABSTRACT CARDS ONLY

No. of Copies	Organization
1	NorthCarolina State College Department of Engineering Raleigh, North Carolina Attn: Prof. R. M. Pinkerton
1	Ohio State University Aeronautical Engineering Dept. Columbus, Ohio Attn: Prof. G. L. von Eschen
1	Pennsylvania State College Dept. of Aeronautical Engineering State College, Pennsylvania Attn: Prof. M. Lessen
1	Polytechnic Institute of Brooklyn Aerodynamic Laboratory 527 Atlantic Avenue Freeport, New York Attn: Dr. A. Ferri
1	Princeton University Forrestal Research Center Princeton, New Jersey Attn: Library
1	Rensselaer Polytechnic Institute Aeronautics Department Troy, New York Attn: Dr. R. P. Harrington
1	University Of Washington Department of Aeronautical Engineering Seattle 5, Washington Attn: Prof. R. E. Street
1	University of Illinois Department of Aeronautical Engineering Urbana, Illinois Attn: Prof. C. H. Fletcher
1	Institute of the Aeronautical Sciences 2 East 64th Street New York 21, New York Attn: Library
1	Professor J. W. Beams Rouse Physical Laboratory University of Virginia Charlottesville, Virginia
1	Professor J. O. Hirschfelder University of Wisconsin Department of Chemistry Madison, Wisconsin